CARBON 65 (2013) 7–12

Available at www.sciencedirect.com

ScienceDirect

journal homepage: www.elsevier.com/locate/carbon

Influence of Cu substrate topography on the growth morphology of chemical vapour deposited graphene ☆

Ye Xiao [a,*], HoKwon Kim [b], Cecilia Mattevi [b], Manish Chhowalla [c], Robert C. Maher [a], Lesley F. Cohen [a]

[a] Blackett Laboratory, Imperial College, Prince Consort Rd, London SW7 2BZ, UK
[b] Materials Department, Imperial College, Exhibition Rd, London SW7 2AZ, UK
[c] Department of Materials Science and Engineering, Rutgers University, Taylor Rd, NJ 08854, USA

ARTICLE INFO

Article history:
Received 13 December 2012
Accepted 28 June 2013
Available online 8 July 2013

ABSTRACT

Raman spectroscopic maps were used to study the local properties of graphene films as grown on corrugated copper foils, by chemical vapour deposition, and after transfer onto SiO_2(300 nm)/Si substrates. Analysis of the Raman peaks show the films exhibit a striped periodic pattern of single- and bi-layer graphene. By performing simultaneous AFM–Raman line maps of the as grown film on Cu we find that the layer growth shows a strong correlation to substrate topography. As a result, compressively strained non-AB stacked bi-layer graphene forms preferentially along the ridges, whilst single-layer graphene grows inside the trenches, of the Cu foil topography. These experimental results suggest that surface mobility is not the dominating factor determining control of layer number in such growth regimes.

1. Introduction

The development of large area growth methods is essential for graphene applications. One of the most promising routes is the growth of graphene by chemical vapour deposition (CVD) on Cu [1]. Recently, Bae et al. [2] demonstrated Cu roll-to-roll based CVD fabrication producing graphene films of up to 30 inches in size showing that Cu based CVD offers significant promise. Sheet resistances were measured at $\approx 100\ \Omega\ sq^{-1}$ with optical transparencies of >97% and carrier mobilities of $\approx 7350\ cm^2\ V^{-1}\ s^{-1}$.

The currently accepted growth mechanism for Cu based CVD graphene is surface based catalytic decomposition whereby a gaseous source of carbon, usually methane (CH_4), is catalytically converted into graphene at high temperatures (in excess of 1000 °C) in what initially appeared to be a self-limiting process as first demonstrated by Li et al. [1], although few layer growth has since been demonstrated by high pressure CVD processes [3].

Here we use simultaneous Raman spectroscopy and atomic force microscope (AFM) topographical mapping of the same area to examine the physical properties of graphene films as grown on corrugated Cu foils and after transfer to SiO_2/Si substrates. By examination of the Raman peak positions, widths and relative intensity ratios, as well as interference enhanced optical images of the film on SiO_2/Si and SEM imaging, we

* *Corresponding author.*
E-mail address: ye.xiao@imperial.ac.uk (Y. Xiao).

0008-6223/$ - see front matter
http://dx.doi.org/10.1016/j.carbon.2013.06.090

determine that the Cu substrate topography is being imprinted in the resultant layer number growth.

2. Experimental methods

2.1. Growth details

In the present study all graphene samples were grown under the same growth conditions using 25 μm thick polycrystalline Cu foils as the growth substrates. An overview of the growth process is given in Ref. [4]. In brief, the Cu foils were first cleaned by sonication in acetone and again in methanol. The Cu foils were then annealed, to increase grain size and remove copper oxide, in a quartz tube furnace for 30 min at 1000 °C with a H_2 flow of 5 sccm in 0.2 mbar low vacuum. Methane was then flowed into the furnace for a period of 30 min. The flow rate was kept at 26.65(CH_4)/12.35(H_2) sccm and the growth pressure was 0.4 mbar. The samples were cooled down to room temperature in the furnace with a H_2 flow rate of 5 sccm. Samples were transferred to SiO_2(300 - nm)/Si substrates by first spin coating a thin layer of poly(-methyl methacrylate) (PMMA) on top of the graphene film. The Cu substrate was removed using a $FeCl_3$ wet chemical etch and the graphene film was transferred onto SiO_2(300 - nm)/Si substrates followed by etching of PMMA in acetone.

2.2. Raman spectroscopy

In this study we use a Renishaw 2000 spectrometer with an attached Leica DMLM confocal microscope fitted with a 50× objective. Raman mapping was performed with a 514 nm laser with a 1.5 μm diameter spot size and 2.3 mW at the focal point and maps of $81 \times 81\ \mu m^2$ were created with a 3 μm pixel resolution.

Raman spectroscopy has become one of the main methods to characterise graphene quality, layer number, strain and doping. Here we review the key features before discussing the properties of our samples. Pristine single-layer graphene (SLG) exhibits two distinct Raman peaks called the G and 2D peaks, found around ~1585 and ~2680 cm^{-1} respectively. The presence of a defect in the honeycomb lattice or at a sample edge is required to activate the D peak and D′ peak, which are found around ~1350 and ~1610 cm^{-1} respectively. Defect density analysis can usually be performed by examining the $I_{D/G}$ ratio. This ratio can be used to estimate the size of sp^2 domains using the Tuinstra–Koenig relation [5,6] although this will not be considered further here.

The ratio between the 2D and G peak can be used, with various caveats, as a guide to layer number [7]. For CVD graphene average values of $I_{2D/G} \approx 2.8$ and 1.2 have been reported for single- and bi-layer graphene (BLG) respectively

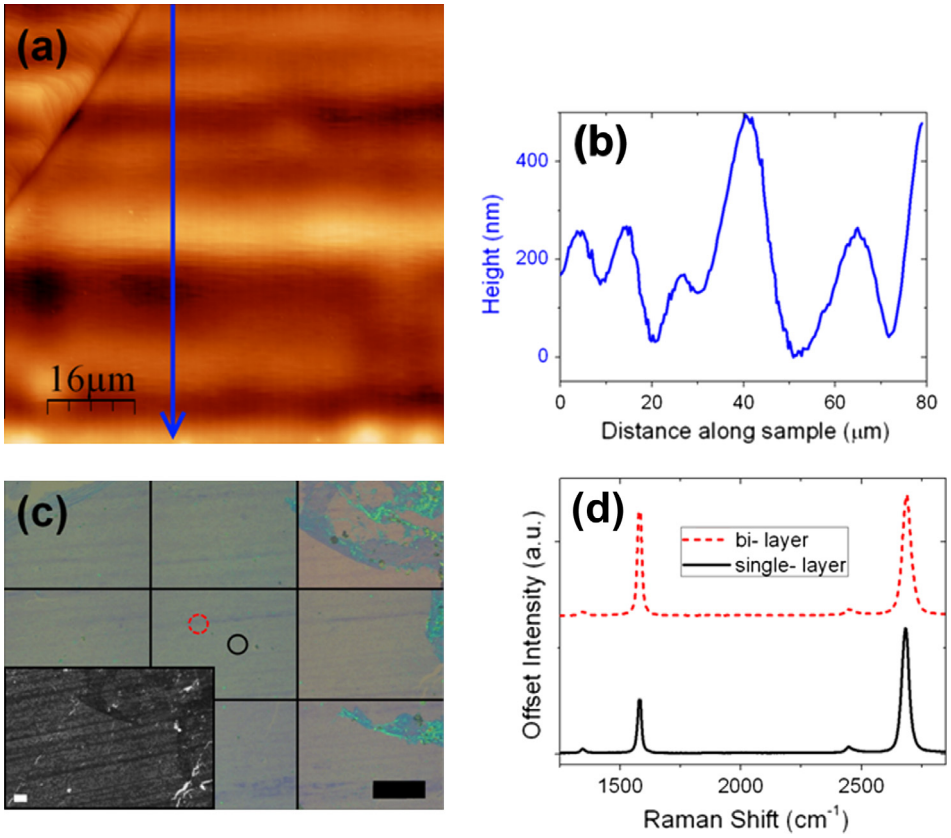

Fig. 1 – (a) AFM map of a typical Cu growth substrate, (b) height profile taken along the arrow in the AFM map showing corrugations of ~200–400 nm in magnitude with a pitch of ~10–20 μm, (c) 50× optical image of typical graphene film transferred on to SiO_2(300 nm)/Si, the inset shows an SEM image of the same area, (d) Raman spectra of single- (solid line) and bi-layer (dashed line) graphene taken from single- (solid circle) and bi-layer (dashed circle) regions of graphene identified by optical contrast on the SiO_2(300 nm)/Si substrate.

Table 1 – List of graphene films investigated, grown on corrugated 25 μm Cu, showing the averaged G and 2D peak positions both on Cu and after transfer to SiO_2(300 nm)/Si.

Sample	G peak position (cm^{-1})		2D peak position (cm^{-1})	
	On Cu	On SiO_2/Si	On Cu	On SiO_2/Si
S1	–	1580 ± 1	–	2681 ± 4
S2	1591 ± 4	–	2704 ± 10	–
S3	1592 ± 3	1582 ± 1	2712 ± 10	2686 ± 2

[1] (note that these are quite different values to those found for mechanically exfoliated graphene (MEG) [7]). Having the $I_{2D/G}$ ratio within a certain range is a necessary condition to determining layer number but not sufficient, as the absolute value has also been shown to be sensitive to carrier doping [8]. Changes in the width and shape of the 2D peak are an additional indicator of layer number, however, this analysis has become more involved as different types of bi-layer stacking have been shown to produce distinct Raman signatures [9]. Both Ni et al. [10] and Poncharal et al. [11] have shown that different types of bi-layer graphene can exist; Bernal (AB) stacked bi-layer graphene, misoriented bi-layer graphene and folded graphene. For mechanically exfoliated AB stacked bi-layer graphene various groups [12,13] have used the evolution of the π electron band structure to explain the change in the composition of the 2D peak from a single Lorentzian peak, for SLG, to four Lorentzian peaks for BLG. Whilst a similar observation has been made for bi-layer CVD graphene the evolution of the 2D peak is far less distinct [14,15] and in some examples the 2D peak has been shown to retain a single Lorentzian composition for $n = 2$ layers with a blueshift in the peak position, indicating non-AB stacked bi-layer graphene. So in summary the $I_{2D/G}$ ratio as well as the 2D peak shape and width can be used in combination to identify layer number and in some cases stacking type.

2.3. *Simultaneous AFM–Raman*

Simultaneous AFM–Raman measurements were performed using a Nanonics MultiView 2000 AFM stage coupled with our Renishaw system. Elongated chrome cantilever tips were purchased from Nanonics. The AFM was operated in tapping mode and set to map $80 \times 80\ \mu m^2$ areas across the samples, Raman spectra were collected at intervals of 0.9 μm. The system was operated such that the AFM tip was positioned at the centre of the Raman beam, both the tip and the beam were kept in a fixed position whilst a piezo driven stage was used to move the sample.

3. Results

Fig. 1(a) shows the topography typical of all the 25 μm thick Cu substrates used. From the height profile shown in Fig. 1(b) we see Cu foils exhibit rolling features, consisting of a series of ridges and trenches of around 200–400 nm deep with a pitch of approximately 10–20 μm.

An optical and SEM image of the same area of a graphene film transferred from Cu to SiO_2(300 nm)/Si is shown in Fig. 1(c). Single- and bi-layer graphene can be distinguished by contrast in both the optical and SEM image and we observe the pattern of rolling features to have been imprinted in the resultant layer growth. Fig. 1(d) shows Raman spectra collected from single- (solid circle) and bi-layer regions identified in the optical image in Fig. 1 (d). We observe the $I_{2D/G}$ ratio to behave as expected with a value of ≈1.2 representing bi-layer regions and ≈2.5 representing single-layer graphene. The observation of rolling features in the layer growth of graphene was consistent across three sets of samples (S1–3) all grown under the same growth conditions. Furthermore, taking the average positions of the G and 2D peaks show both peaks to be blueshifted on Cu with respect to their values after transfer to SiO_2(300 nm)/Si as summarised by Table 1.

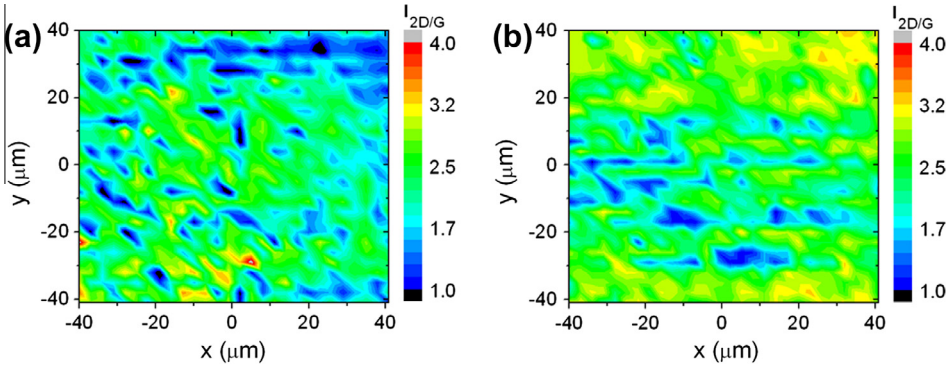

Fig. 2 – Raman map of the $I_{2D/G}$ ratio for sample S3 showing a vertically striped pattern of single- (green) and bi-layer growth (blue) on both (a) Cu and after transfer to, (b) SiO_2(300 nm)/Si. (For interpretation of the references to colour in this figure legend, the reader is referred to the web version of this article.)

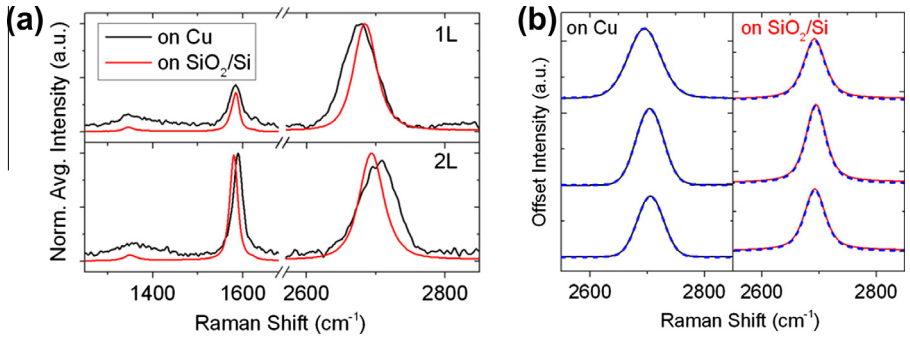

Fig. 3 – (a) Normalised and averaged Raman spectra taken from areas of single- and bi-layer graphene on both Cu and after transfer to SiO_2(300 nm)/Si, (b) single Lorentzian fits to three sets of 2D peaks representative of bi-layer regions on both substrates.

Fig. 2 shows Raman mapping of sample S3, both on Cu and after transfer to SiO_2(300 nm)/Si. We observe the rolling pattern present in the topography, optical and SEM images we have shown so far to also be present in the $I_{G/2D}$ ratio maps, which we have demonstrated to be a valid indicator of layer number. We observe that single-layer coverage ($I_{2D/G} \geqslant 1.7$) is $\geqslant$80% for the graphene film both on the Cu and on the SiO_2(300 nm)/Si.

Fig. 3(a) shows the Raman spectra from single- and bi-layer regions both on Cu and after transfer to SiO_2(300 nm)/Si for sample S3. Here we compare averaged and normalised spectra from both single- and bi-layer regions on both substrates. The fitting of single Lorentzian peaks to three sets of representative spectra from bi-layer regions on both substrates is shown in Fig. 3(b). We show that in all cases our 2D peaks can be fitted with single Lorentzian functions, as opposed to the four Lorentzian fittings associated with AB stacked bi-layer graphene, implying that the bi-layer regions are not AB stacked.

To determine the relationship between Cu substrate topography and layer growth more accurately we performed simultaneous AFM–Raman measurements over two different areas on sample S3 across the line profiles indicated on the AFM maps shown in Fig. 4(a) and (b). Fig. 4(c) and (d) shows

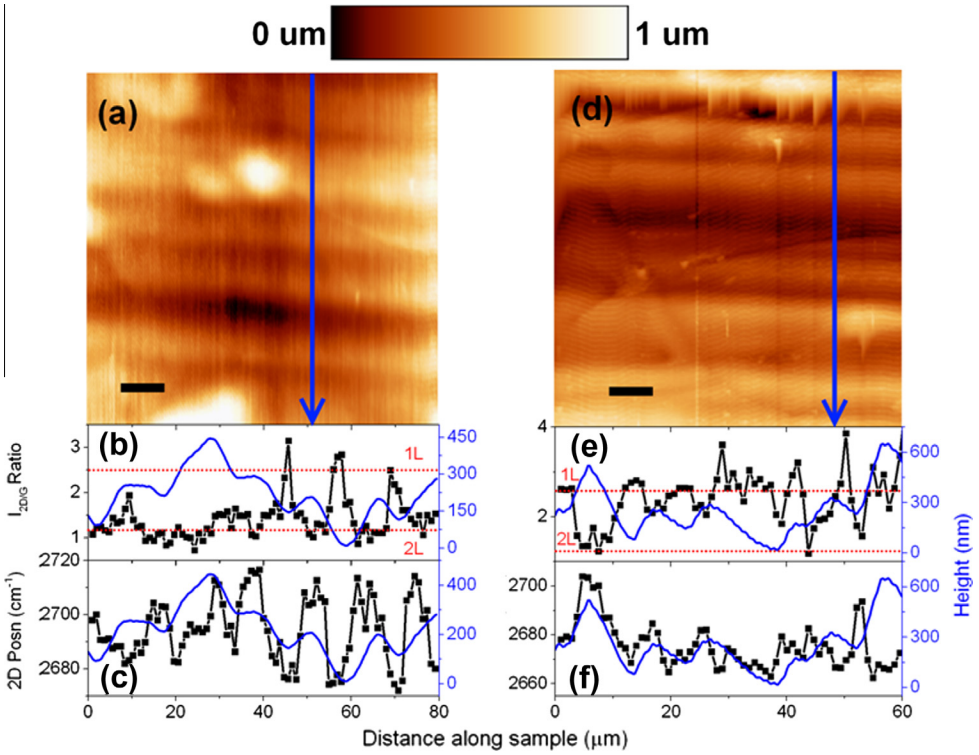

Fig. 4 – (a, d) AFM maps taken over two different areas of sample S3 when on Cu (b and c, e and f) simultaneous AFM–Raman line profiles taken over the arrows indicated in (a, d) respectively showing the correlation between both the (b, e) $I_{2D/G}$ ratio and the (c, f) 2D peak position with topography. The dotted red lines are labelled to represent regions of predominantly single- and bi-layer graphene. (For interpretation of the references to colour in this figure legend, the reader is referred to the web version of this article.)

the correlation between both the $I_{2D/G}$ ratio and the 2D peak position with the underlying topography. We have highlighted regions of single- and bi-layer graphene as determined from the $I_{2D/G}$ ratio.

4. Discussion

Our observation of rolling features in the resultant growth of our graphene films, shown in Fig. 1, is consistent across the numerous samples. Similar growth patterns have been reported by various other groups for topographically similar substrates [16–18]. Coupled with reports of homogenous large area single-layer graphene growth on smooth electro-polished Cu foil [17,19] our work supports the general premise that topography plays a key role in the resulting graphene film properties.

As previously stated, the $I_{2D/G}$ ratio cannot be used in isolation to determine layer number as doping effects must be taken into account. However, given that we can confirm the presence of single- and bi-layer regions, both optically and from SEM imaging, which can be correlated to the Raman spectra taken from both regions, as shown in Fig. 1, we conclude that for our samples the $I_{2D/G}$ ratio is a valid indication of layer number and that doping effects are insignificant.

From Fig. 2 we can see the rolling features in the resultant growth to be already present in the as grown graphene on Cu. We can therefore conclude that our observed bi-layer regions are not due to folding of the film during the transfer process to SiO_2(300 nm)/Si substrates, but rather originate from the seeding of bi-layer growth as a result of the corrugated topography of the growth substrate. Further information about the physical properties of the single- and bi-layer regions can be extracted from the averaged Raman spectra of both areas as shown in Fig. 3. Closer examination of the peak positions show that both the G and 2D peaks are redshifted, on Cu compared to SiO_2(300 nm)/Si, for single-layer graphene and blue-shifted for bi-layer. We attribute this shift to the formation of compressively strained bi-layer graphene and tensile strained single-layer graphene. The relaxation of both types of strain is evidenced by the reduction of the G (28–23 cm^{-1}) and 2D (55–41 cm^{-1}) peak widths when transferred off Cu. Different strain environments are indicative of a topographic influence. From Table 1 we see that the averaged G and 2D peak positions redshift for graphene films when transferred off Cu to SiO_2(300 nm)/Si substrates, we attribute this net shift to the relaxation of compressive strain which is well understood to have originated from differences in the thermal expansion coefficient between Cu and graphene during the growth process [20]. However, in Fig. 4(c) and (f) we see that there is a clear correlation of the 2D peak position of a graphene film with the topography of the underlying Cu substrate. This suggests that whilst thermal mismatch strain is dominant in our samples there is also a measureable contribution from topography.

The seeding of multilayer growth from scratches and copper grain boundaries on polished Cu surfaces and the existence of multilayer stripe-like islands of graphene on unpolished copper have been previously reported [22]. The latter being attributed to the surface morphology of unpolished Cu. But no previous work has studied this growth in detail. Theoretically, Luo et al. [17] propose that free carbon radicals propagating along corrugated surfaces would become trapped in trenches as a result of reduced surface mobility and form turbostatic bi-/few-layer graphene. This would result in the formation of single-layer graphene along the tops of ridges and bi-layer graphene within the trenches of a corrugated surface. Indeed, this has been observed at lower growth temperatures ($T < 870$ °C) and was associated with the reduced surface mobility of carbon radicals due to local surface roughness in corrugated Cu foils [21]. Kim et al. have provided a detailed description of the growth mechanism for the formation of graphene nuclei. They showed the growth limiting factor to be primarily dependent on the availability of carbon radicals at the growing front of a graphene nucleus and that, for low temperature regimes ($T < 870$ °C), the lifetime of such carbon radicals is dominated by their surface mobility [21]. Here we extend upon that work to look at the growth mechanism in the high temperature regime, specifically $T = 1000$ °C. Fig. 4(b), (c), (e) and (f) show the simultaneous AFM–Raman measurements of two different areas of a graphene film (sample S3) when still on Cu. Both sites exhibit a clear correlation between topography and bi-layer seeding. Our results imply that the growth of a second layer of graphene responds to the curvature of the substrate surface. In Fig. 4(b) and (e) we observe that bi-layer seeding corresponds to areas of positive curvature (i.e. along the tops of ridges) in contradiction to the low temperature growth regime. This observation is not surprising given that for high temperature regimes the lifetime of carbon radicals is reported to be determined by the desorption rate rather than surface mobility. Indeed, our observation of bi-layer seeding is similar to that of few-layer growth at step edges (which also have positive curvature) which is due to the preferential attachment of carbon at such sites. In addition, the solubility of carbon in Cu can increase for surfaces of high positive curvature due to the Kelvin–Gibbs effect [22]. As such, our results suggest that increased nucleation along the ridges occurs, leading to bi-layer growth, due to the increased likelihood of critical supersaturation of carbon radicals at such sites which is consistent with our previous observations on these samples [21].

5. Summary

In this study we have shown the correlation between corrugated substrate topography and the seeding of bi-layer growth. We have also identified that for high temperature growth (at 1000 °C), bi-layer growth seeds in the trenches of the copper substrate, indicating that surface mobility is not the dominating factor determining control of layer number under the growth conditions employed in this study.

Acknowledgements

This work was supported by the Leverhulme Trust, the EPSRC and Imperial College. We would like to thank Sam Ladak for assistance with the atomic force microscopy images of the Cu foil and Stefan Maier for useful scientific discussion.

REFERENCES

[1] Li X, Cai W, An J, Kim S, Nah J, Yang D, et al. Large-area synthesis of high-quality and uniform graphene films on copper foils. Science 2009;324(5932):1312–4.

[2] Bae S, Kim H, Lee Y, Xu X, Park J-S, Zheng Y, et al. Roll-to-roll production of 30-inch graphene films for transparent electrodes. Nat Nanotechnol 2010;5(8):574–8.

[3] Bhaviripudi S, Jia X, Dresselhaus MS, Kong J. Role of kinetic factors in chemical vapour deposition synthesis of uniform large area graphene using copper catalyst. Nano Lett 2010;10(10):4128–33.

[4] Mattevi C, Kim H, Chhowalla M. A review of chemical vapour deposition of graphene on copper. J Mater Chem 2011;21(10):3324–34.

[5] Tuinstra F, Koenig JL. Raman spectrum of graphite. J Chem Phys 1970;53(3):1126–30.

[6] Ferrari AC, Robertson J. Resonant Raman spectroscopy of disordered, amorphous, and diamondlike carbon. Phys Rev B 2001;64(7):075414.

[7] Graf D, Molitor F, Ensslin K, Stampfer C, Jungen A, Hierold C, et al. Spatially resolved Raman spectroscopy of single- and few-layer graphene. Nano Lett 2007;7(2):238–42.

[8] Casiraghi C, Pisana S, Novoselov KS, Geim AK, Ferrari AC. Raman fingerprint of charged impurities in graphene. Appl Phys Lett 2007;91(23):233108.

[9] Lui CH, Li Z, Chen Z, Klimov PV, Brus LE, Heinz TF. Imaging stacking order in few-layer graphene. Nano Lett 2010;11(1):164–9.

[10] Ni Z, Wang Y, Yu T, Shen Z. Raman spectroscopy and imaging of graphene. Nano Res 2008;1(4) [273-91-91].

[11] Poncharal P, Ayari A, Michel T, Sauvajol JL. Raman spectra of misoriented bilayer graphene. Phys Rev B 2008;78(11):113407.

[12] Ferrari AC, Meyer JC, Scardaci V, Casiraghi C, Lazzeri M, Mauri F, et al. Raman spectrum of graphene and graphene layers. Phys Rev Lett 2006;97(18):187401.

[13] Park JS, Reina A, Saito R, Kong J, Dresselhaus G, Dresselhaus MS. G′ band Raman spectra of single, double and triple layer graphene. Carbon 2009;47(5):1303–10.

[14] Yan K, Peng H, Zhou Y, Li H, Liu Z. Formation of bilayer bernal graphene: layer-by-layer epitaxy via chemical vapour deposition. Nano Lett 2011;11(3):1106–10.

[15] Lee S, Lee K, Zhong Z. Wafer scale homogeneous bilayer graphene films by chemical vapour deposition. Nano Lett 2010;10(11):4702–7.

[16] Vlassiouk I, Regmi M, Fulvio P, Dai S, Datskos P, Eres G, et al. Role of hydrogen in chemical vapour deposition growth of large single-crystal graphene. ACS Nano 2011;5(7):6069–76.

[17] Luo Z, Lu Y, Singer DW, Berck ME, Somers LA, Goldsmith BR, et al. Effect of substrate roughness and feedstock concentration on growth of wafer-scale graphene at atmospheric pressure. Chem Mater 2011;23(6):1441–7.

[18] Han GH, Güneş F, Bae JJ, Kim ES, Chae SJ, Shin H-J, et al. Influence of copper morphology in forming nucleation seeds for graphene growth. Nano Lett 2011;11(10):4144–8.

[19] Zhang B, Lee WH, Piner R, Kholmanov I, Wu Y, Li H, et al. Low-temperature chemical vapour deposition growth of graphene from toluene on electropolished copper foils. ACS Nano 2012;6(3):2471–6.

[20] Yu V, Whiteway E, Maassen J, Hilke M. Raman spectroscopy of the internal strain of a graphene layer grown on copper tuned by chemical vapour deposition. Phys Rev B 2011;84(20):205407.

[21] Kim H, Mattevi C, Calvo MR, Oberg JC, Artiglia L, Agnoli S, et al. Activation energy paths for graphene nucleation and growth on Cu. ACS Nano 2012;6(4):3614–23.

[22] Nasibulin AG, Queipo P, Shandakov SD, Brown DP, Jiang H, Pikhitsa PV, et al. Studies on mechanism of single-walled carbon nanotube formation. J Nanosci Nanotechnol 2006;6(5):1233–46.